



Constraining Progenitors of Observed LMXBs Using CARB Magnetic Braking



Constraining Progenitors of Observed LMXBs Using CARB Magnetic Braking
 Kenny X. Van, Natalia Ivanova
 University of Alberta, Edmonton, AB, T6G 2R3, Canada



Introduction

When searching for binary systems based on orbital parameters, it is one of the main ways to find observed binary systems. The number of simulated progenitor systems is very important.

This work uses an improved magnetic braking scheme that is more accurate than the commonly used standard prescription. The improved and standard magnetic braking schemes are compared to reproduce the observed LMXBs.

↓

Observed LMXBs

To determine the effectiveness of the standard magnetic braking scheme, we must compare simulated results to observed systems. We have compiled a table of observed progenitor LMXBs at a range of periods to test our magnetic braking prescription. Table 1 is a table of the observed systems and the period, mass, and mass transfer rate ranges we use in our comparison. Choosing all these physical parameters at the same time is necessary to effectively constrain progenitor binaries.

System Name	$\log(P[\text{days}])$	$\log(M[\text{sol}])$	$\log(\dot{M}[\text{sol/yr}])$
1E1501-540	1.935-1.940	0.95-0.98	1.45-1.48
1E1601-500	1.934-1.935	0.95-0.98	1.45-1.48
1E1740-404	1.935-1.937	0.95-0.98	1.45-1.48
1E1800-01	1.880-1.875	0.95-0.98	1.45-1.48
1E1812-07	1.881-1.875	0.95-0.98	1.45-1.48
1E1838-07	1.875-1.880	0.95-0.98	1.45-1.48
1E1840-03	1.880-1.875	0.95-0.98	1.45-1.47

Other period: 1E1630-506 (1.832-1.775), 0.91-0.94, 1.45-1.48
 1E1640 (1.876-1.775), 0.95-0.98, 1.45-1.48
 1E1745-404 (1.875-1.680), 0.95-0.98, 1.42-1.75
 1E1822-07 (1.880-1.680), 0.95-0.98, 1.75-1.8

Intermediate period: 1E1812-07 (1.881-1.875), 0.91-0.98, 1.75-1.8
 1E1838-07 (1.880-1.885), 0.95-0.98, 1.75-1.8

Long period: 1E1812-07 (1.881-1.680), 0.95-0.98, 1.75-1.8

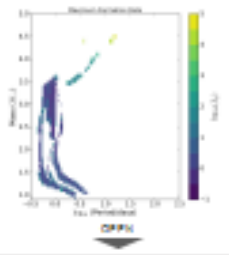
*Table 1: A selection of progenitor systems with ...

↓

Estimated Progenitor Rates

By requiring our simulations to match in initial period, mass transfer rate and mass ratio simultaneously, we can solve for the progenitor rate of our 14 observed LMXBs. We estimate the required progenitor birth rate using the formula $\lambda_{\text{progenitor}} = \dots$

Using the prescription, it identifies a given observed LMXB. N is the number of observed systems, λ is the initial mass and period, T is the birth rate, C is the area of the bin and τ is the amount of time the simulation spent in the observed bin. Due to each observed system being unique, N is always 1 for each LMXB. We estimate a maximum rate for a given progenitor bin, via assuming that the observed LMXB is produced by a single combination of initial donor mass and period.



↓

Progenitor Structure

The figure plotting the maximum formation rate estimates in each bin clearly shows some structure.

- Unobserved systems (LMXBs) seen only as produced by simulations where the initial period is near the observed period. The progenitors of 1E1838-07 and 1E1840-03 make up the large majority of the progenitor space.
- The short-period systems all have initial periods shorter than LMXB progenitors. The progenitors of 1E1630-506 and 1E1640-01 make up the large majority of systems seen around 2 solar masses. The progenitors of 1E1630-506 and 1E1640-01 result in the short period source ...

↓

Conclusions

- Our improved magnetic braking prescription successfully reproduces our sample of observed LMXBs.
- The progenitors of the observed LMXBs show some structure characteristic to the ...

Kenny X. Van, Natalia Ivanova

University of Alberta, Edmonton, AB, T6G 2R3, Canada



PRESENTED AT:



INTRODUCTION

Mass transfer in binary systems results in emitted radiation which is one of the main ways we can observe binary systems. The number of well-observed, persistent binaries is very limited[1,3,6].

This work focuses on an improved magnetic braking scheme which we have derived that is more physically motivated than the commonly used Skumanich prescription. Our Convection and Rotation Boosted (CARB) magnetic braking scheme accounts for additional physical parameters and is not scaled to match with main sequence G type stars.

Using MESA[5], we ran a large grid of donor masses and periods to simulate binary systems. We apply our magnetic braking scheme to produce results that span our entire parameter space. We compare these simulated systems to observed binaries to determine possible progenitors of observed persistent LMXBs.

CARB MAGNETIC BRAKING DERIVATION

This research uses our Convection and Rotation Boosted (CARB) magnetic braking scheme. To derive this we first assume spherical symmetry, which results in the angular momentum lost

$$\dot{J}_{\text{MB}} = -\frac{2}{3}\Omega\dot{M}_{\text{W}}R_{\text{A}}^2$$

This shows that the magnetic braking depends only on the amount of mass lost through winds and the Alfvén radius. Unfortunately both of these quantities are not well known. We can make some assumptions about the physical properties of the system to change the equation to be a function of different properties. Assuming a radial magnetic field,

$$\left(\frac{R_{\text{A}}}{R}\right)^2 = \frac{B_{\text{s}}^2 R^2}{4\pi R_{\text{A}}^2 \rho_{\text{A}} v_{\text{A}}^2} = \frac{B_{\text{s}}^2 R^2}{\dot{M}_{\text{W}} v_{\text{A}}}$$

Here we have equations describing how the Alfvén radius relates to the surface magnetic field strength, the radius of the star, the wind mass-loss rate and the velocity of the wind at the Alfvén surface. Using energy conservation, we can convert this velocity to scale with the escape velocity

$$\frac{v_{\text{A}}}{v_{\text{esc}}} = \left(\frac{R}{R_{\text{A}}}\right)^{1/2}$$

In the case when the star and its attached magnetic field rotate, the regular stellar wind can also be additionally accelerated by the time it reaches the Alfvén radius. Reville et al. 2015 parametrized the additional acceleration by replacing the surface escape velocity with a modified velocity, which includes the effects of rotation [8]. Using this variable allows us to rewrite our equation for the Alfvén radius as

$$\left(\frac{R_{\text{A}}}{R}\right)^3 = \frac{B_{\text{s}}^4 R^4}{\dot{M}_{\text{W}}^2} \times \frac{1}{v_{\text{esc}}^2 + 2\Omega^2 R^2 / K_2^2}$$

This equation has an additional K constant which controls the limit where the rotation rate begins to play a significant role. Using simulations it has been found that K should be approximately 0.07 [8]. In this approach, the Alfvén radius shrinks as the rotation rate increases, weakening the angular momentum loss in fast rotating binaries. Plugging this form of the Alfvén radius into the angular momentum equation gives a new prescription for angular momentum loss,

$$\dot{J}_{\text{MB}} = -\frac{2}{3}\Omega\dot{M}_{\text{W}}^{1/3} R^{14/3} B_{\text{s}}^{8/3} (v_{\text{esc}}^2 + 2\Omega^2 R^2 / K_2^2)^{-2/3}$$

Substituting a convective turnover scaling relation for the magnetic field strength of the star we get the modified magnetic braking prescription used in our simulations,

$$\begin{aligned} \dot{J}_{\text{MB}} = & -\frac{2}{3}\dot{M}_{\text{W}}^{1/3} R^{14/3} (v_{\text{esc}}^2 + 2\Omega^2 R^2 / K_2^2)^{-2/3} \\ & \times \Omega_{\odot} B_{\odot}^{8/3} \left(\frac{\Omega}{\Omega_{\odot}}\right)^{11/3} \left(\frac{\tau_{\text{conv}}}{\tau_{\odot,\text{conv}}}\right)^{8/3} \end{aligned}$$

OBSERVED LMXBS

To determine the effectiveness of the derived magnetic braking scheme, we must compare simulated results to observed systems. We have compiled a table of observed persistent LMXBs at a range of periods to test our magnetic braking prescription. Below is a table of our observed systems and the period, mass ratio, and mass transfer rate ranges we use in our comparison. Matching all three physical parameters at the same time is necessary to effectively constrain progenitor binaries.

System Name	$\log_{10}(P/\text{day})$	q	$\log_{10}(\dot{M}_a)$
UCXB			
4U 0513-40	[-1.95, -1.90]	[0.01, 0.06]	[-9.0, -8.4]
2S 0918-549	[-1.94, -1.89]	[0.01, 0.06]	[-9.6, -8.4]
4U 1543-624	[-1.92, -1.87]	[0.01, 0.06]	[-8.9, -8.4]
4U 1850-087	[-1.86, -1.81]	[0.01, 0.06]	[-9.8, -8.2]
M15 X-2	[-1.82, -1.77]	[0.01, 0.06]	[-9.5, -8.9]
4U 1626-67	[-1.55, -1.50]	[0.01, 0.06]	[-9.5, -8.4]
4U 1916-053	[-1.48, -1.43]	[0.03, 0.08]	[-9.4, -8.7]
Short period			
4U 1636-536	[-0.82, -0.77]	[0.15, 0.40]	[-8.9, -8.4]
GX 9+9	[-0.78, -0.73]	[0.20, 0.33]	[-8.5, -8.0]
4U 1735-444	[-0.73, -0.68]	[0.29, 0.48]	[-8.2, -7.7]
2A 1822-371	[-0.65, -0.60]	[0.26, 0.36]	[-7.6, -7.1]
Intermediate period			
Sco X-1	[-0.12, -0.07]	[0.15, 0.58]	[-7.8, -7.1]
GX 349+2	[-0.05, 0.00]	[0.39, 0.65]	[-7.8, -7.1]
Long period			
Cyg X-2	[0.97, 1.02]	[0.25, 0.53]	[-7.8, -7.0]

Table 1. A collection of persistent LMXBs with observed periods, mass ratios, and mass transfer rates. The ranges span the errors of each quantity and is centered on the observed value.

As a first check, we will plot our simulated data in 2D with the axis being period and mass transfer rate.

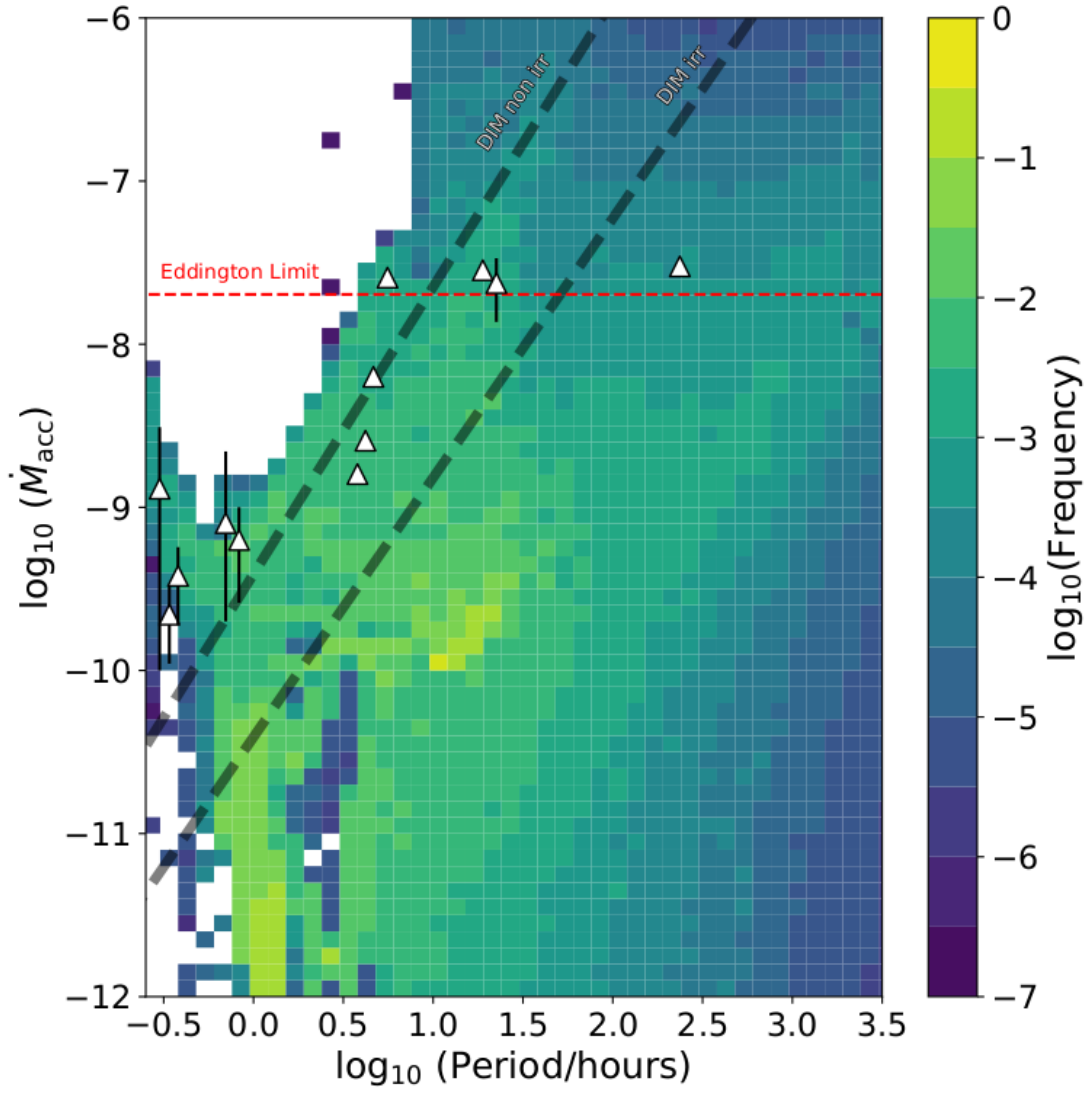


Figure 1. A figure showing the relative probability of finding a simulated system in a given bin in period-mass transfer rate space. The symbols used to represent the observed LMXBs from table 1 with the appropriate errors. The two gray dashed lines show a model that predicts the divide between persistent and transient systems. Persistent systems are predicted to lie above the line.

ESTIMATED PROGENITOR RATES

By requiring our simulations to match in orbital period, mass transfer rate and mass ratio simultaneously, we were able to find progenitors for each of our 14 observed LMXBs. We estimate the required progenitor birth rate using the formula:

$$N_{\text{obs}}^k = \sum_{ij} \frac{df_{ij}}{dA_{ij}} \Delta A^k \tau_{ij}^k$$

Where the superscript k denotes a given observed LMXB, N is the number of observed systems, i and j are the initial mass and period, f is the birth rate, A is the area of the bin and τ is the amount of time the simulation spent in the observed bin. Due to each observed system being unique, N is always 1 for each LMXB. To estimate a maximum rate for a given progenitor bin, we assume that the observed LMXB is produced by a single combination of initial donor mass and period.

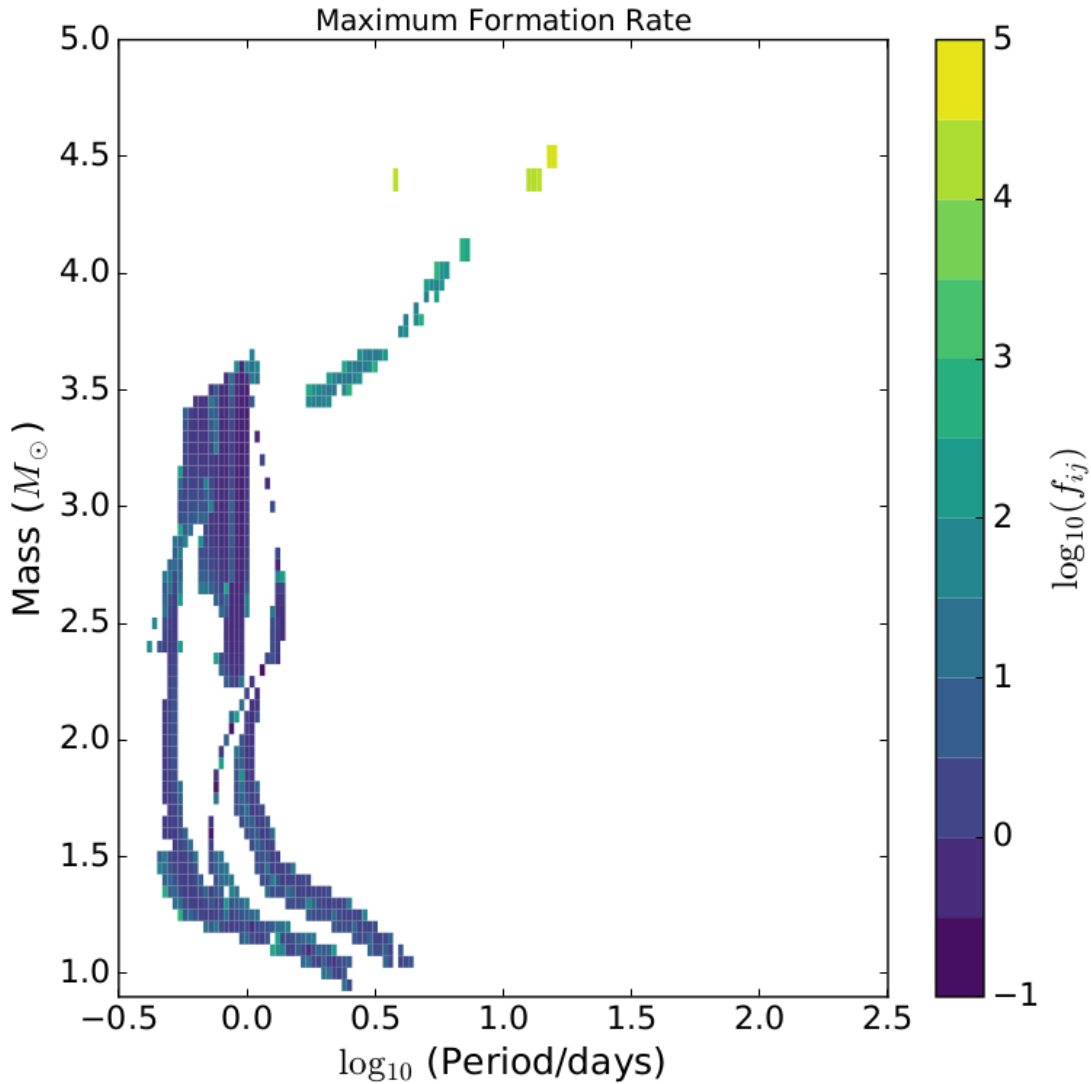


Figure 2. The maximum calculated LMXB formation rate as calculated using our equation. The plot contains progenitors for the observed LMXBs from table 1. We calculate a formation rate per bin if a single bin can reproduce multiple observed LMXBs the larger rate is shown.

The maximum calculated birth rate for each of our observed LMXBs is given in the following table:

System Name	$\log_{10}(P/\text{day})$	$M_i(M_{\odot})$	$\log_{10}(f_{ij})$
UCXB			
4U 0513-40	-0.08	1.3	2.19
2S 0918-549	-0.08	1.3	1.49
4U 1543-624	0.16	1.2	1.62
4U 1850-087	-0.12	1.75	1.25
M15 X-2	-0.12	1.75	1.04
4U 1626-67	0.34	1.1	2.05
4U 1916-053	-0.1	1.9	2.37
Short period			
4U 1636-536	-0.12	2.35	2.46
GX 9+9	-0.18	2.85	2.06
4U 1735-444	-0.26	1.25	2.85
2A 1822-371	-0.26	2.9	2.56
Intermediate period			
Sco X-1	-0.02	1.85	2.08
GX 349+2	0.14	2.7	2.34
Long period			
Cyg X-2	1.2	4.5	4.62

Table 2. The mass, period and formation rate of the maximum rate calculated using our model. We do not currently account for results that reproduce multiple observed LMXBs in our equation.

PROGENITOR STRUCTURE

The figure plotting the maximum formation rate estimated in each bin clearly shows some structure.

- Ultra-compact systems (UCXB) can only be produced by simulations where the initial period is near the bifurcation period. The progenitors of UCXBs make up the narrow curve in the parameter space.
- The short-period systems all have initial periods shorter than UCXB progenitors. The progenitors of 4U 1636-536 and GX 9+9 make up the large grouping of systems seen around 3 solar masses. The progenitors of 4U 1735-444 and 2A 1822-371 result in the short period curve spanning from 1 to 2.5 solar masses. This suggests that despite similar observed quantities these two sets of binaries have very different origins.
- The intermediate period binaries are produced by the curved shape at periods above the bifurcation period. There is a significant overlap between the progenitors Sco X-1 and GX 349+2. There is overlap between the higher mass progenitors of GX 349+2 and the UCXB progenitors which means that GX 349+2 may one day evolve into a UCXB.
- There is little structure in long period systems. Among our results, the progenitors of Cyg X-2 require the highest birth rate. This suggests that it is very difficult to reproduce this observed binary.

CONCLUSIONS

- Our improved magnetic braking prescription successfully reproduces our sample of observed LMXBs
- The progenitors of the observed LMXBs show some structure that needs to be investigated further
- Preliminary results suggest that it is difficult to reproduce Cyg X-2

AUTHOR INFORMATION

Kenny X. Van

Ph.D. Candidate in Astrophysics

Department of Physics

CCIS 2-108, University of Alberta

Website: <https://kvan1231.github.io/>

Email: Kvan@ualberta.ca

ABSTRACT

We present a new method for constraining the mass transfer evolution of low mass X-ray binaries (LMXBs) -- a reverse population synthesis technique. This is done using the detailed 1D stellar evolution code MESA (Modules for Experiments in Stellar Astrophysics) to evolve a high-resolution grid of binary systems spanning a comprehensive range of initial donor masses and orbital periods. We use our modified magnetic braking scheme the CARB (Convection And Rotation Boosted) magnetic braking prescription. The CARB magnetic braking scheme has been shown to effectively reproduce a sample of well studied persistent LMXBs with observed mass ratios, periods and mass transfer rates. Using the reverse population synthesis technique -- where we follow any simulated system that successfully reproduces an observed LMXB backwards, we can constrain possible progenitors for each observed binary. This technique can be applied to any observed LMXB with well-constrained mass ratios, period and mass transfer rate. With the upcoming GAIA DR3 containing information on binary systems, this technique can be applied to the data release and act as an independent method to compare to the results found using normal population synthesis.

REFERENCES

- [1] Heinke C. O., Ivanova N., Engel M. C., Pavlovskii K., Sivakoff G. R., Cartwright T. F., Gladstone J. C., 2013, *ApJ*, 768, 184
- [2] Justham, S., Rappaport, S., & Podsiadlowski, P. 2006, *MNRAS*, 366, 1415
- [3] Liu Q. Z., van Paradijs J., van den Heuvel E. P. J., 2007, *A&A*, 469, 807
- [4] Pavlovskii K., Ivanova N., 2016, *MNRAS*, 456, 263
- [5] Paxton B., et al., 2019, arXiv e-prints, p. arXiv:1903.01426
- [6] Podsiadlowski P., Rappaport S., Pfahl E. D., 2002, *ApJ*, 565, 1107
- [7] Rappaport S., Verbunt F., Joss P. C., 1983, *ApJ*, 275, 713
- [8] Réville V., Brun A. S., Matt S. P., Strugarek A., Pinto R. F., 2015, *ApJ*, 798, 116